Monthly Notices of the ROYAL ASTRONOMICAL SOCIETY

MNRAS **528,** 3464–3472 (2024) https://doi.org/10.1093/mnras/stae226
Advance Access publication 2024 January 22

Chemical clocks and their time zones: understanding the [*s*/Mg]–age relation with birth radii

Bridget Ratcliffe [1]★ Ivan Minchev [1] Gabriele Cescutti [2,3,4] Emanuele Spitoni,[3] Henrik Jönsson [5] Friedrich Anders,[6,7,8] Anna Queiroz[1,9,10] and Matthias Steinmetz[1]

[1]*Leibniz-Institut für Astrophysik Potsdam (AIP), An der Sternwarte 16, D-14482 Potsdam, Germany*
[2]*Dipartimento di Fisica, Sezione di Astronomia, Università di Trieste, via G. B. Tiepolo 11, I-34143 Trieste, Italy*
[3]*INAF, Osservatorio Astronomico di Trieste, via G.B. Tiepolo 11, I-34131 Trieste, Italy*
[4]*INFN, Sezione di Trieste, Via A. Valerio 2, I-34127 Trieste, Italy*
[5]*Materials Science and Applied Mathematics, Malmö University, SE-205 06 Malmö, Sweden*
[6]*Dept. de Física Quàntica i Astrofísica (FQA), Universitat de Barcelona (UB), C Martí i Franqués, 1, E-08028 Barcelona, Spain*
[7]*Institut de Ciències del Cosmos (ICCUB), Universitat de Barcelona (UB), C Martí i Franqués, 1, E-08028 Barcelona, Spain*
[8]*Institut d'Estudis Espacials de Catalunya (IEEC), C Gran Capità, 2-4, E-08034 Barcelona, Spain*
[9]*Laboratório Interinstitucional de e-Astronomia – LIneA, Rua Gal. José Cristino 77, Rio de Janeiro RJ-20921-400, Brazil*
[10]*Institut für Physik und Astronomie, Universität Potsdam, Haus 28 Karl-Liebknecht-Str 24/25, D-14476 Golm, Germany*

Accepted 2024 January 4. Received 2023 December 4; in original form 2023 July 20

ABSTRACT

The relative enrichment of *s*-process to α-elements ([*s*/α]) has been linked with age, providing a potentially useful avenue in exploring the Milky Way's chemical evolution. However, the age–[*s*/α] relationship is non-universal, with dependencies on metallicity and current location in the Galaxy. In this work, we examine these chemical clock tracers across birth radii ($R_{\rm birth}$), recovering the inherent trends between the variables. We derive $R_{\rm birth}$ and explore the [*s*/α]–age–$R_{\rm birth}$ relationship for 36 652 APOGEE DR17 red giant and 24 467 GALAH DR3 main-sequence turn-off and subgiant branch disc stars using [Ce/Mg], [Ba/Mg], and [Y/Mg]. We discover that the age–[*s*/Mg] relation is strongly dependent on birth location in the Milky Way, with stars born in the inner disc having the weakest correlation. This is congruent with the Galaxy's initially weak, negative [*s*/Mg] radial gradient, which becomes positive and steep with time. We show that the non-universal relations of chemical clocks is caused by their fundamental trends with $R_{\rm birth}$ over time, and suggest that the tight age–[*s*/Mg] relation obtained with solar-like stars is due to similar $R_{\rm birth}$ for a given age. Our results are put into context with a Galactic chemical evolution model, where we demonstrate the need for data-driven nucleosynthetic yields.

Key words: stars: abundances – Galaxy: abundances – Galaxy: disc – Galaxy: evolution.

1 INTRODUCTION

Chemical abundances are connected to a star's age and place of birth (Freeman & Bland-Hawthorn 2002; Ratcliffe et al. 2022), providing an effective tool in analysing the Milky Way's evolutionary history. In particular, recent works have utilized the link between abundances and age to estimate stellar ages for large samples of red giant branch stars (Hayden et al. 2022; Anders et al. 2023; Ciucă et al. 2023; Leung et al. 2023), where traditional methods fail or only provide ages for small samples in select fields. While these abundance-driven ages have improved our understanding of important evolutionary events, some of the models can be quite complex, and may not capture the precise nature of the abundance–age relationship.

Over the past few years, the ratio between *s*-process and α-elements ([*s*/α]) has been found to be linearly related with age in Milky Way solar-like stars (Nissen 2015; Nissen et al. 2020b) and giants (Slumstrup et al. 2017), as well as in other galaxies (Skúladóttir et al. 2019). Understanding this link between [*s*/α] and age could provide a way to examine chemical evolution by omitting the dependencies in modelling age. The negative correlation between [*s*/α] and age is driven by the differing time scales to synthesize the two elements, as α-elements are created during supernovae II (SNII) which happen on fast time-scales, while *s*-process elements are produced in the asymptotic giant branch (AGB) phase of low- and intermediate-mass stars which happens on a slower time-scale (Karakas & Lattanzio 2014; Matteucci 2021, and references within). The relative differences in the time-scales suggests the possibility that the [*s*/α][1] abundance can be an age indicator, or chemical clock (Nissen 2015; Spina et al. 2016; Tucci Maia et al. 2016).

Using only 25 solar-like stars, da Silva et al. (2012) found a correlation between [*s*/α] and age, which has successfully been

★ E-mail: bratcliffe@aip.de

[1]The most common chemical clock is [Y/Mg] or [Y/Al], though similar trends are found across other *s*-process and α-elements.

replicated with more stars in other works using solar-type stars in the solar neighbourhood (Nissen 2015, 2016; Tucci Maia et al. 2016; Titarenko et al. 2019; Jofré, Jackson & Tucci Maia 2020; Nissen et al. 2020b). However, its dependency on location in the Galaxy (Casali et al. 2020; Casamiquela et al. 2021; Viscasillas Vázquez et al. 2022) and metallicity (Delgado Mena et al. 2017; Feltzing et al. 2017; Sales-Silva et al. 2022) is an ongoing question. Quantifying this radial dependency is a non-trivial task, as stars radially migrate away from their birth sites (Sellwood & Binney 2002; Roškar et al. 2008; Schönrich & Binney 2009; Minchev & Famaey 2010; Frankel et al. 2020), blurring fundamental chemical relations (e.g. Ratcliffe et al. 2023).

Recently, works have utilized the homogeneity of birth clusters (Bland-Hawthorn, Krumholz & Freeman 2010) to estimate stellar birth radii ($R_{\rm birth}$) directly from their metallicities and ages. In order to assign a specific [Fe/H] and age to a birth location, the relationship between age, birth radius, and [Fe/H] over time needs to be known. While this relationship can be modelled (Frankel et al. 2018), more recent works have proposed methods which require less assumptions. In order to derive $R_{\rm birth}$, Minchev et al. (2018) recovered the metallicity evolution in the Galactic disc over time by enforcing the resulting $R_{\rm birth}$ distributions to remain physically meaningful. More recently, Lu et al. (2022) discovered a linear relation between the scatter in [Fe/H] for a given age and the [Fe/H] gradient evolution with time, allowing for the evolution of the metallicity gradient to be recovered with minimal assumptions (see Ratcliffe et al. 2024 for limitations). Applying this method to Apache Point Observatory Galactic Evolution Experiment (APOGEE; Majewski et al. 2017) DR17, Ratcliffe et al. (2023) derived $R_{\rm birth}$ for 145 447 red giant stars to recover the time evolution of chemical abundances across the Milky Way disc, revealing the information lost when only considering the radial gradient evolution estimated using current radius. That work put in context (and quantified) the expectation from models and simulations that radial mixing has significantly distorted present-day chemo–kinematical relations used for inferring the Milky Way formation history (e.g. Minchev et al. 2012; Pilkington et al. 2012; Kubryk, Prantzos & Athanassoula 2013; Minchev, Chiappini & Martig 2014; Vincenzo & Kobayashi 2020).

In this work, we explore the universality of chemical clocks across birth radii for giants and main-sequence turn-off and subgiant branch (MSTO + SGB) disc stars in the Milky Way. In particular, we examine how the age–[*s*/Mg] relationship differs across the Galaxy after minimizing the effect of radial migration. Section 2 presents the data sets used in this analysis. Section 3 gives the results and discussion of our findings in relation to previous works. In particular, the radial [*s*/Mg] gradient across time and the enrichment of [*s*/Mg] over time at different birth radii are given in Sections 3.1 and 3.2, respectively. Section 3.3 illustrates why tight age–[*s*/Mg] relations are found in solar twins, and we interpret our results in Section 3.4 using a Galactic chemical evolution model that is independent of our $R_{\rm birth}$ estimates. Our conclusions are given in Section 4.

2 DATA

We examine three *s*-process elements – Ce, Ba, and Y – to study the relationship between [*s*/Mg], age, and birth radii. We use the [Ce/Fe] abundance from the Brussels Automatic Code for Characterizing High-accuracy Spectra (BACCHUS; Masseron, Thibault, and Hawkins 2016) Analysis of Weak Lines in APOGEE Spectra (BAWLAS; Hayes et al. 2022) catalogue, and pair it with [Fe/H] and [Mg/Fe] abundances from APOGEE DR17 (Majewski et al. 2017; Abdurro'uf et al. 2022) of the fourth phase of the Sloan Digital Sky Survey (SDSS-IV; Blanton et al. 2017), which are processed using the APOGEE Stellar Parameter and Chemical Abundance Pipeline (ASPCAP; Holtzman et al. 2015; García Pérez et al. 2016; Jönsson et al. 2020). We partner these abundances with spectroscopic stellar ages from Anders et al. (2023) and guiding radii ($R_{\rm guide}$) calculated as

$$R_{\rm guide} = R_{\rm gal} V_\phi / V_0,$$

where V_ϕ and $R_{\rm gal}$ are the Galactocentric azimuthal velocity and Galactocentric cylindrical radius from the astroNN catalogue (Leung & Bovy 2019), and $V_0 = 229.76$ km s^{-1} is the Milky Way rotation curve at solar radius (Schönrich, Binney & Dehnen 2010; Bovy et al. 2012). To ensure that we select a high quality sample, we use APOGEE red giant ($2 < \log g < 3.6, 4\,250 \leq T_{\rm eff} \leq 5\,500$ K) disc ($|z| < 1$ kpc, eccentricity <0.5, $|$[Fe/H]$| < 1$) stars with unflagged abundances, [Fe/H]$_{\rm err} < 0.015$, age$_{\rm err} < 1.5$ Gyr, SNR > 100, age < 12 Gyr, $|$[Ce/Fe]$| \leq 1$, and [Ce/Fe]$_{\rm err} < 0.07$ dex.

We additionally use the [Y/Fe], [Ba/Fe], [Mg/Fe], and [Fe/H] abundance measurements provided in Galactic Archaeology with HERMES (GALAH; De Silva et al. 2015) DR3 (Buder et al. 2021), with ages from the STARHORSE value-added catalogue (Queiroz et al. 2023), which was recently corrected in a new version[2] $R_{\rm guide}$ is again calculated from cylindrical rotational velocity, with kinematics from the dynamics value-added catalogue. For our GALAH MSTO + SGB disc ($|$[Fe/H]$| < 1$, eccentricity <0.5, $|z| < 1$ kpc) sample, we perform similar cuts as above; we keep stars with unflagged abundances, $|$[X/Fe]$| < 1$, [Fe/H]$_{\rm err} < 0.1$, age$_{84}$ − age$_{16} < 2.5$ Gyr, `snr_c2_iraf` > 50, 2 < age < 12 Gyr, and [X/Fe]$_{\rm err} < 0.1$ dex.

We estimate a star's birth radius directly from their [Fe/H] and age measurements

$$R_{\rm birth}(\text{age}, [\text{Fe/H}]) = \frac{[\text{Fe/H}] - [\text{Fe/H}](R = 0, \tau)}{\nabla[\text{Fe/H}](\tau)}, \quad (1)$$

using the birth metallicity gradient (∇[Fe/H](τ)) and central metallicity evolution over cosmic time τ ([Fe/H]($R = 0, \tau$)) from Ratcliffe et al. (2023). Equation (1) results from the recently discovered empirical relation that recovers the Milky Way disc metallicity evolution with radius and cosmic time directly from the data, which is inverted to recover stellar birth radii as a function of age and [Fe/H], with no use of Galactic chemical evolution modelling (Lu et al. 2022; Ratcliffe et al. 2023). As described in those works, the derived gas metallicity gradient starts relatively flat and steepens strongly to ≈ -0.15 dex kpc^{-1} during the Gaia–Sausage–Enceladus event (Belokurov et al. 2018; Helmi et al. 2018); over the next nine or so Gyr, the gradient flattens to today's value, while exhibiting small oscillations possibly due to gas accretion events (Buck et al. 2023; Ratcliffe et al. 2023). While recovered directly from the data using [Fe/H] and age measurements only, this temporal gradient evolution is consistent with inside-out disc formation models, as known since the seminal work by Matteucci & Francois (1989).

We correct for the 0.05 dex systematic offset in [Fe/H] between GALAH and APOGEE (Buder et al. 2021) before calculating $R_{\rm birth}$ for our GALAH sample. Since the main goal of this work is to look at overall trends with $R_{\rm birth}$ between [*s*/Mg] and age, and not to directly compare the numerical relationships between catalogues, we do not correct for other potential offsets. To get the [*s*/Mg] abundance, we simply subtract [Mg/Fe] from [*s*/Fe]. After performing the quality

[2] https://data.aip.de/projects/aqueiroz2023.html

cuts listed above and removing stars with $R_{\rm birth} < 0$, we are left with 36 652 APOGEE giants and 24 467 GALAH MSTO + SGB stars.

3 RESULTS AND DISCUSSION

With estimates of stellar ages and birth radii for large samples of stars, we can analyse the properties of chemical clocks over lookback time – which is not the same as age, see e.g. Ratcliffe et al. (2023) – and assess the effect of radial migration by comparing these properties to observed trends with guiding radii.

3.1 Radial gradient evolution

Using our $R_{\rm birth}$ estimates, we find distinct trends between [s/Mg] and $R_{\rm birth}$ in the top panels of Fig. 1, where the $R_{\rm birth}$–[s/Mg] relation illustrates the time evolution of [s/Mg] abundance gradients. In particular, we find that for all three of our [s/Mg] relations, the youngest mono-age populations have a steep positive radial gradient, while the oldest mono-aged populations have a weaker radial gradient. In fact, the three oldest age groups correspond to the high-α sequence (see Anders et al. 2023; Queiroz et al. 2023), which appear to have a slightly negative [s/Mg] radial birth gradient.

Once the low-α sequence began forming, the [s/Mg] radial gradient began quickly steepening with time. This steepening in the radial gradient visualized in the top panels of Fig. 1 can be interpreted as a rapid increase in the enrichment with Galactic radius. While variations in star formation efficiency, radial gas flows, and a variable initial mass function can contribute to abundance gradient development, this steepening can be explained as an effect of radial migration. The production of the s-process elements occurs during the AGB phase, which gives sufficient time for migration to proceed. The larger fraction of s-process elements at larger radius is then due to low- and intermediate-mass AGB stars migrating before polluting the interstellar medium. Indeed, it is well-established (Minchev, Chiappini & Martig 2014; Frankel et al. 2020) that outside $\sim$1 disc scale length ($\sim$3.5 kpc; Bland-Hawthorn & Gerhard 2016), stars migrate larger distances outward and contribute more to a given radius. The steep [s/Mg] radial gradient for the youngest populations also explains the scatter in [s/Mg] found in young (<2 Gyr) open clusters (Peña Suárez et al. 2018; Casali et al. 2020), as there is a range of [s/Mg] values throughout the disc for a given (younger) age.

The bottom row of Fig. 1 presents the $R_{\rm guide}$–[s/Mg] plane for mono-age populations, illustrating the differences in measuring the radial [s/Mg] gradients with $R_{\rm birth}$ (top row) and $R_{\rm guide}$ (bottom row). Similar to Ratcliffe et al. (2023), we find that the observed radial gradients with $R_{\rm guide}$ are weaker than the radial birth gradients, showing the level to which radial migration masks fundamental trends. Particularly for [Ba/Mg] and [Y/Mg] (GALAH sample), the $R_{\rm guide}$–[s/Mg] relation has a minor correlation overall. [Ce/Mg] (APOGEE sample) shows similar trends, however due to the larger spatial coverage, the younger aged populations show a positive radial slope which is only hinted at in the GALAH sample.

3.2 Enrichment with cosmic time

While the [s/Mg] radial gradient can provide insights into how the relative fraction of s-process to α-elements varies across the disc with time, the age–[s/Mg] relation is potentially a useful tool in estimating stellar age that needs better understanding. Previous works have found that the age–[s/α] relation changes as a function of current radius, suggesting that the differences arise from the strong, non-monotonic dependence of the s-process yields with metallicity and different star formation histories (Casali et al. 2020). However, due to radial mixing processes, a given location in the Galaxy is comprised of stars born in a range of Galactic radii (depending on the age; see e.g. Minchev et al. 2018; Agertz et al. 2021).

The top panels of Fig. 2 show the age–[s/Mg] relation for stars born at different locations in the Galaxy. We find that most mono-$R_{\rm birth}$ populations increase in [s/Mg] before flattening out and seeing minimal differences in [s/Mg] at later times. The flattening occurs at increasingly younger age for larger radii, which can be linked to the disc inside-out growth. In our data sets, the larger $R_{\rm birth}$ bins do not show a weakening in the age–[s/Mg] gradient due to the lack of younger stars. This trend is consistent across red giants ([Ce/Mg]) and MSTO + SGB stars ([Ba/Mg], [Y/Mg]), and is in disagreement with previous work that found the age–[s/Mg] relation to be weaker in field giants and stronger in dwarfs (Katime Santrich et al. 2022). This shows that once working with $R_{\rm birth}$, the differences among different stellar evolutionary states is minimized. Given that each birth radius has a similar trend in enrichment of [s/Mg], this suggests that the effect of star formation is simply to shift the trends to larger radii as the disc grows with time.

In contrast to the top panels of Fig. 2, the bottom row shows the age–[s/Mg] relation for stars in different guiding, rather than birth, radial bins. We find that the well-defined self-similar trends seen for the mono-$R_{\rm birth}$ populations are now strongly blurred and largely overlapping. In particular, the flattening for younger ages at a given radius is almost completely lost, especially for [Ba/Mg] and [Y/Mg], except for a hint in the innermost $R_{\rm guide}$ bin.

Using open clusters, Viscasillas Vázquez et al. (2022) found that [Ba/Mg] and [Y/Mg] have respectively a weak and inverted trend with age in the inner disc. Using birth radii, we find that both [Ba/Mg] and [Y/Mg] have a weakly positive relation with age for smaller $R_{\rm birth}$. In fact, we find the mono-$R_{\rm birth}$ populations behave similarly for all three elements (albeit with different slopes) in the [s/Mg]–age plane, which differs from previous findings reporting that [Y/Mg] and [Ba/Mg] have different trends (e.g. da Silva et al. 2012), and shows the additional information gained using birth radii. Recently, Casali et al. (2023) showed that stars located in outer regions of the disc lie on steeper slopes in the age–[Ce/α] plane than stars currently located more inwards. Our work agrees with this finding, with our Fig. 1 illustrating that this is caused by a more intense enrichment of [s/Mg] in the outer disc.

As mentioned in Section 3.1, the [s/Mg] radial gradient has been strengthening with time. In both our GALAH and APOGEE samples, the valley between the high- and low-α sequences happens between 9 and 10 Gyr ago, suggesting that chemical clocks behave differently for the two sequences. The validity of chemical clock indicators using s-process elements in the high-α sequence has been questioned before, with arguments that AGB stars would not have produced enough s-process elements that quickly (Hayden et al. 2022). However, we see in Fig. 2 that these older stars have the strongest correlation with age, showing minimal differences across the different mono-$R_{\rm birth}$ populations. This also contrasts the differences between using current and birth radius, as the age–[s/Mg] relation has been found to be flat for older stars (Casali et al. 2023). One way to interpret this is that as the disc evolved, factors – such as radial migration processes – caused a variation in the production of [s/Mg] as a function of radius, therefore creating a spread in [s/Mg] abundance for a given age which increased with time. We explore these factors in Section 3.4 using Galactic chemical evolution modelling.

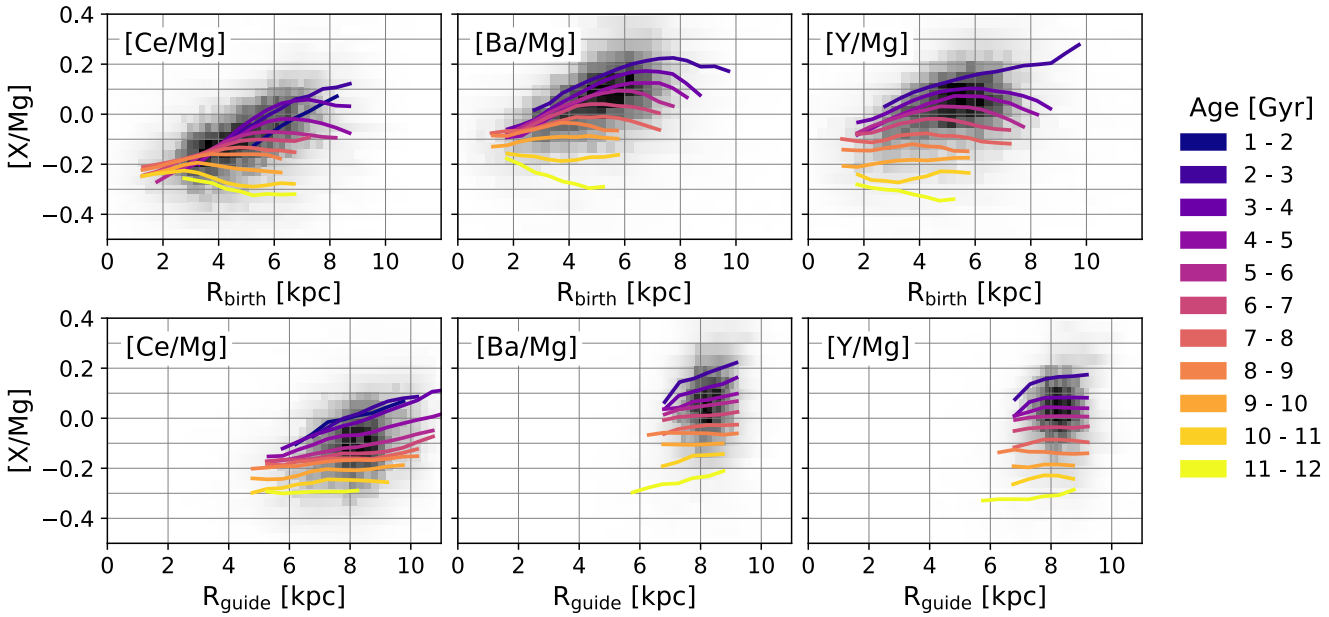

Figure 1. Time evolution of [*s*/Mg] abundance gradients for our APOGEE ([Ce/Mg]) and GALAH ([Ba/Mg], [Y/Mg]) samples. *Top*: Running means of different mono-age populations, determined by calculating the average [*s*/Mg] for $R_{\rm birth}$ bins of width 0.5 kpc and then smoothed over 1 kpc. Note, that age here becomes lookback time, since we are using $R_{\rm birth}$. *Bottom*: Same as the top panels, but looking at the variation over age with $R_{\rm guide}$. [*s*/Mg] has a weak relationship with $R_{\rm birth}$ for older aged stars, which becomes positive and stronger with decreasing lookback time. Over time, the outer disc enriches in [*s*/Mg] faster than the inner disc due to AGB stars migrating outwards before polluting the interstellar medium.

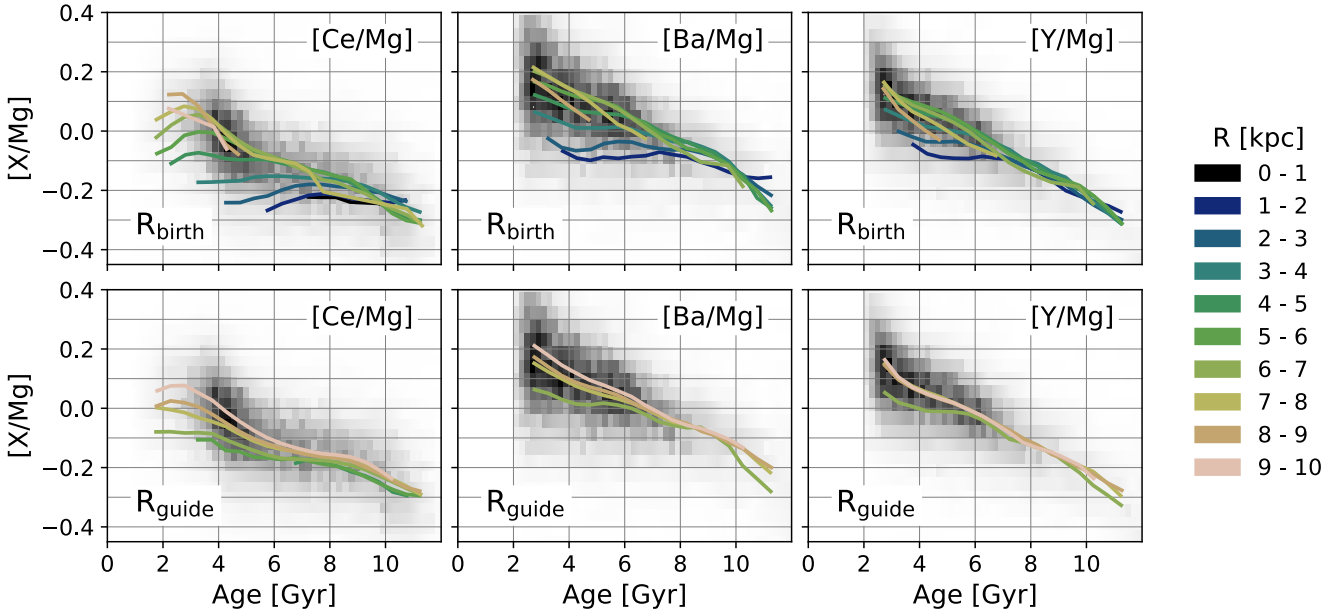

Figure 2. The age–[*s*/Mg] plane of [Ce/Mg] (APOGEE), [Ba/Mg] (GALAH), and [Y/Mg] (GALAH) overlaid by the running means of *top*: mono-$R_{\rm birth}$ populations and *bottom*: mono-$R_{\rm guide}$ populations. The running means are measured by calculating the average [*s*/Mg] for age bins of 0.5 Gyr and smoothing over 1 Gyr. The smaller $R_{\rm birth}$ tracks show a weak relationship with age while the correlation between [*s*/Mg] and age becomes quite strong for larger $R_{\rm birth}$. Each $R_{\rm birth}$ sees a similar trend with [*s*/Mg] over time; a radius sees an initial increase in [*s*/Mg] until it flattens and stays nearly constant with time until the present day. This trend is drastically different than looking at mono-$R_{\rm guide}$ groups, which show minimal differences beyond slightly steeper slopes for outer radii.

3.3 Tight age–[*s*/Mg] relationship in solar twins is driven by varying birth radii

The tight relation between [*s*/Mg] and age found for solar twins in e.g. Nissen (2015), Tucci Maia et al. (2016), and Nissen et al. (2020b) led to the attempt of expanding this relation to larger samples. While some works have not found a metallicity dependence (Titarenko et al. 2019), others have noted a dependence on [Fe/H] when examining larger regions of the Galaxy, suggesting that the linear relation between age and chemical clocks is limited by [Fe/H] (Feltzing et al. 2017; Delgado Mena et al. 2019). For example Casali et al. (2020) found that lower-[Fe/H] stars had a higher correlation between [Y/α] and age, while the higher [Fe/H] stars had the weakest slope in the age–[Y/α] plane.

Since $R_{\rm birth}$, [Fe/H], and age are directly linked, it is natural that the differences across metallicity described above are potentially driven by varying $R_{\rm birth}$. Indeed, for a given age, the higher [Fe/H] stars have smaller $R_{\rm birth}$, which are the birth radii with the weakest age–[*s*/Mg] relation. Another way to think of this is that the lower metallicity stars come from a wider variety of $R_{\rm birth}$ (see the right panel of fig. 2 in Ratcliffe et al. 2023), and therefore run through more mono-$R_{\rm birth}$ populations in Fig. 2 faster than the higher [Fe/H] stars. The dependency on [Fe/H] therefore seems to be due to looking at stars born in different places of the Milky Way.

What does this mean for the samples of solar-like stars that show tight relations between age and [*s*/Mg]? Fig. 3 shows the age–[Y/Mg] and age–[Sr/Mg] planes for the 72 nearby solar-type stars provided in Nissen et al. (2020b), coloured by their derived $R_{\rm birth}$. It is clear that there is a gradient with $R_{\rm birth}$ in these planes for this sample, with younger stars having larger $R_{\rm birth}$ and older stars having lower $R_{\rm birth}$. The minor scatter seen about the correlation is due to varying $R_{\rm birth}$ for a given age, which is caused by the variation in [Fe/H] at that age. In other words, the variation in [*s*/Mg] about the chemical clock relation at a given age is due to stars being born at different birth radii. This is especially apparent in [Sr/Mg], which does not show as tight of a correlation with age as [Y/Mg] does.

We find that the four stars that lie off of this tight relation particularly for [Y/Mg] (ζ^1Ret, ζ^2Ret, and the Na-rich stars, marked with black and orange squares, respectively) are born at predominantly different locations than the other stars with similar age in this sample.

3.4 Comparison with Galactic chemical evolution models

To interpret our results, we compare with the age–[*s*/Mg] relationship produced using Galactic chemical evolution (GCE) modelling. We use the same nucleosynthesis adopted in the chemical evolution model by Van der Swaelmen et al. (2023; model D), for what concerns magnesium and the r-process component of barium. The *s*-process component of barium is the same as assumed in Rizzuti et al. (2019), with the *s*-process production of AGB stars taken from the nucleosynthesis prescriptions of Cristallo et al. (2015) and those of massive stars from Frischknecht et al. (2016). The Galactic disc is described as rings of 2 kpc, with a single episode of infall. This is a simplified assumption, compared to a possible double, or even triple, infall (see e.g. Spitoni et al. 2021, 2023). The remaining parameters of chemical evolution such as a radial dependent infall law with an inside-out time-scale, initial mass function, star formation law, total surface mass–density as a function of galactocentric distance and stellar lifetimes are the same as the disc phase considered in Cescutti et al. (2007). These assumptions produce a metallicity gradient flattening with time, as found in Lu et al. (2022) and Ratcliffe et al. (2023).

Unlike massive stars, AGB stars are long-lived and thus have enough time to migrate and pollute neighbouring bins. To account for this effect, we implement radial mixing in a simplified manner by assuming that at each time-step a fixed fraction of 10 per cent of the barium in each ring is transferred to the ring outside. This mimics the enrichment by a percentage of AGB which migrates toward the outskirts of the disc, where they release their *s*-process enrichment; we define this as Model A.

The time evolution of the radial gradient of Model A is presented in the left panel of Fig. 4 (dashed lines). This model captures the overall trend of the [Ba/Mg] radial gradient across time that we find in Fig. 1, i.e. the radial gradient begins negative and becomes positive with time. However, the age–[Ba/Mg] relation for Model A (right panel of Fig. 4, dashed lines) shows significant differences from our observational findings. This model predicts that after the initial pollution the [Ba/Mg] abundance stays relatively constant with time for the outer radii, while in the inner disc its abundance significantly decreases (Fig. 4). This is in strong disagreement with our results in Fig. 2, where we find the [Ba/Mg] abundance in the inner disc stays fairly constant with age and the outer disc sees a steep increase with time.

A possible explanation for the decrease in [Ba/Mg] with time produced in Model A is that the amount of Ba produced in the models of high-metallicity AGB stars is too low. To analyse this solution, we run Model A with a modification to the yields; the Ba yields for $Z > 0.01$ are replaced with the yields of $Z = 0.01$. In our set of nucleosynthesis, the yields of barium at $Z = 0.01$, are about a factor of 2 larger than the yields at $Z = 0.02$, depending on the mass of the AGB considered. The expectations of this modified model (Model B) are shown as the solid lines in Fig. 4. We see that the discrepancies listed above are primarily resolved; i.e. the [Ba/Mg] abundance at each radius stays relatively constant with time after its initial increase. The results of Model B also appear to agree with what concerns the [Ba/Mg] versus $R_{\rm birth}$ plot (solid lines in left panel of Fig. 4), although in this plane the difference imposed by the variation in the yields are less significant. We underline that with our data it is not trivial to disentangle possible enrichment of *s*-process elements happening in binary systems. In this scenario, if the primary ended its life at AGB, the secondary star could be enhanced in *s*-process elements; at the same time, the mass transfer can bias the determination of the age towards younger ages. Further investigations are needed to understand the impact of this population that at this stage we consider negligible.

The results that we found for [Ba/Mg] can be explained by a disc with a decreasing exponential surface density where the inner part enriches faster due to higher star formation efficiency and an inside-out time-scale for the disc formation. This combined with a strong metallicity dependence in the yields of *s*-process, with a mild modification of the most metal-rich tail, and with a migration of around 10 per cent of the AGB products can explain the trends found in the data. The results of this section are robust to different values of this migration percentage, with a smaller/larger fraction causing smaller/larger variations in [*s*/Mg] across $R_{\rm birth}$ for younger ages. Choosing the optimal fraction is non-trivial and outside the scope of this work. However, at least with these simplified assumptions, the migration needed is mild.

We acknowledge that the model does not perfectly reproduce the data as there are many parameters in modelling the Milky Way's evolution. However, despite the numerous GCE models in the literature, we are not aware of any that predict the steepening of [*s*/Mg] with time that we find. Given that AGB stars are a main contributor to *s*-process elements, and that radial migration

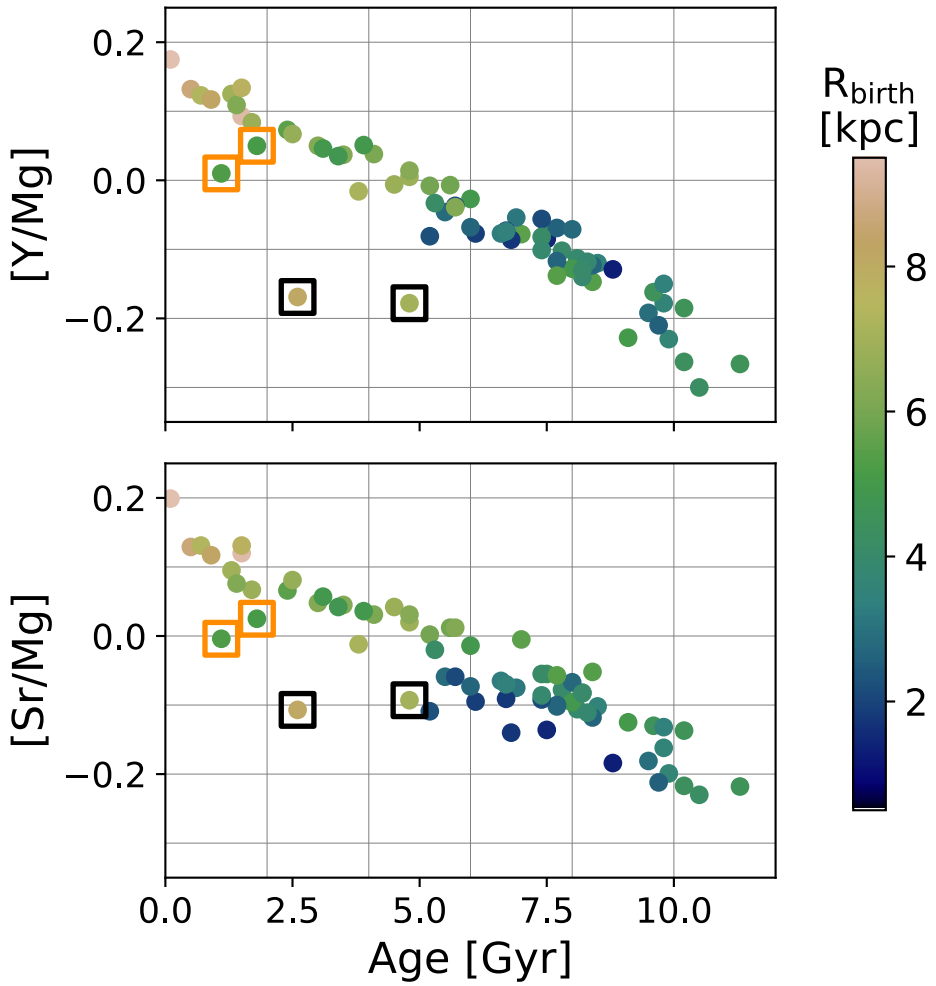

Figure 3. *Top*: The age–[Y/Mg] and *bottom*: age–[Sr/Mg] relation of 72 nearby solar-like stars presented by Nissen et al. (2020b). Stars are coloured by their estimated R_{birth}. The linear [Y/Mg] and [Sr/Mg] relations with age results from stars with different R_{birth} across age, with the general trend of younger stars born at larger radii. The main deviants from this line [the components of ζ Retucili (black squares; outliers with lower [Y/Mg]) and the two Na-rich stars (orange squares; outliers with higher [Y/Mg]) are due to their differing birth location compared to other stars at a similar age. This figure illustrates that scatter about the chemical clock relation is a result of a sample containing stars born at different radii at a given age.

is unavoidable, it is only natural that we consider this simpler model to get a first-order estimate on the [*s*/Mg] gradient evolution. Indeed, this section shows that our simple model is able to capture the main trends from Figs 1 and 2 and it provides us with an interpretation of our results. This section also shows the power of R_{birth}, and how it can be used to constrain GCE models.

4 CONCLUSIONS

This work investigated the age–[*s*/Mg] relation across R_{birth} using 36 652 APOGEE DR17 red giant disc stars and 24 467 GALAH DR3 MSTO + SGB disc stars. Previous works found variations in chemical clocks with current radius, however due to stars radially migrating away from their birth sites, these fundamental trends can be difficult to interpret. In this work, we explored the relative evolution of *s*-process and α-elements across time and birth radii in the Milky Way to recover the spatially dependent chemical clock relation, and additionally revealed why the [*s*/Mg]–age relationship depends on the stellar sample examined. Our key findings are:

(i) The [*s*/Mg] radial birth gradient for all three elements examined started initially weakly negative, flattened around the time of high- to low-α transition, and then became increasingly positive (or concave downwards) towards redshift zero (Fig. 1). The initially weakly negative gradient could be a result of the initial mass function, while over time the outer disc enriches faster in [*s*/Mg] than the inner disc due to the migration of AGB stars before enriching the interstellar medium with *s*-process elements.

(ii) The age–[*s*/Mg] relation varies across R_{birth}, with each radius seeing an initial increase in [*s*/Mg] before varying little with time (Fig. 2). The enrichment from AGB stars that have migrated outwards causes the increase in [*s*/Mg] abundance at a given radius. Due to inside-out formation, eventually this additional enrichment slows down/stops, causing a radius to have little change in [*s*/Mg] abundance with time. This variation suggests that the scatter about the [*s*/Mg]–age line is predominantly due to samples containing a variety of R_{birth} for a given age.

(iii) When the dispersion in R_{birth} is small for a given age (such as in Milky Way solar-like stars), a tight correlation between [*s*/Mg] and age is found (Fig. 3).

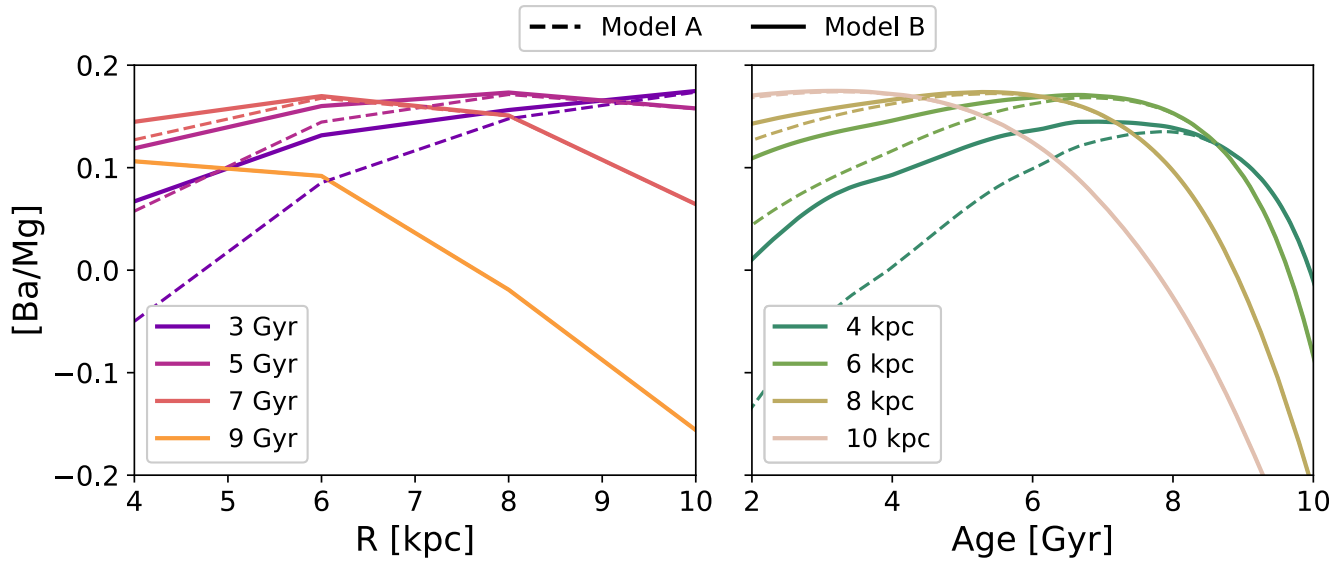

Figure 4. *Left*: [Ba/Mg] versus $R_{\rm birth}$ and *right*: [Ba/Mg] versus age planes using a single-infall GCE model with inside out growth and simple radial migration as described in Section 3.4 (Model A, dashed lines). Model A fails to reproduce the observed relationship between age, [Ba/Mg], and $R_{\rm birth}$. Particularly, the right panel shows that mono-$R_{\rm birth}$ populations see a decline in [Ba/Mg] with decreasing age – unlike the trends shown in Fig. 2. Model B (solid lines), which allows for more production of Ba at higher metallicities in AGB stars, corrects this issue, and is able to capture the overall trends observed with our $R_{\rm birth}$.

(iv) Using a GCE model with standard nucleosynthetic yields, we find that the [Ba/Mg] abundance decreases with time for each mono-$R_{\rm birth}$ population in disagreement with the data. A simple correction for allowing more Ba to be produced at higher metallicities, as well as a simple model of radial migration, address this issue and is able to reproduce the trends found using our $R_{\rm birth}$ estimates (Fig. 4).

Our results explicitly show that there is no universal [s/Mg]–age relation across the Galactic disc, in agreement with previous works (e.g. Viscasillas Vázquez et al. 2022). Here, however, we revealed how this correlation depends on $R_{\rm birth}$ (and thus [Fe/H]), which demonstrates the inherent relationship between [s/Mg] abundance and age in the Milky Way that is not masked by radial migration. In particular, we illustrate how radial migration affects the [s/Mg] radial gradient with time, which in turn creates a variation in the [s/Mg] abundance across birth radii and causes a weaker correlation between age and [s/Mg] for younger ages.

The time evolution of the age–[s/Mg] relation that we uncovered with knowledge of birth radius was used to constrain the metallicity dependence of the AGB yields and the radial migration strength of a simple GCE model – which are typically constrained by only present-day observations with age and radius, and independent of our $R_{\rm birth}$ estimates. Our work also highlights the utility of $R_{\rm birth}$ in understanding the Milky Way disc's chemical evolution, as the contribution from different mechanisms that can affect abundance evolution are all naturally accounted for without prior knowledge or quantification that is needed in chemo–dynamical modelling.

ACKNOWLEDGEMENTS

BR and IM acknowledge support by the Deutsche Forschungsgemeinschaft under the grant MI 2009/2-1. This work was also partially supported by the European Union (ChETEC-INFRA, project number 101008324).

DATA AVAILABILITY

The data sets used and analysed for this study are derived from data released by APOGEE DR17, GALAH DR3, Queiroz et al. (2023) (corrected version: https://data.aip.de/projects/aqueiroz2023.html), Anders et al. (2023), and Nissen et al. (2020a). The rest of the relevant data sets are available from the corresponding author on reasonable request.

REFERENCES

Abdurro'uf et al., 2022, ApJS, 259, 35
Agertz O. et al., 2021, MNRAS, 503, 5826
Anders F. et al., 2023, A&A, 678, A158
Belokurov V., Erkal D., Evans N. W., Koposov S. E., Deason A. J., 2018, MNRAS, 478, 611
Bland-Hawthorn J., Gerhard O., 2016, ARA&A, 54, 529
Bland-Hawthorn J., Krumholz M. R., Freeman K., 2010, ApJ, 713, 166
Blanton M. R. et al., 2017, AJ, 154, 28
Bovy J. et al., 2012, ApJ, 759, 131
Buck T., Obreja A., Ratcliffe B., Lu Y., Minchev I., Macciò A. V., 2023, MNRAS, 523, 1565
Buder S. et al., 2021, MNRAS, 506, 150
Casali G. et al., 2020, A&A, 639, A127
Casali G. et al., 2023, A&A, 677, A60
Casamiquela L., Castro-Ginard A., Anders F., Soubiran C., 2021, A&A, 654, A151
Cescutti G., Matteucci F., François P., Chiappini C., 2007, A&A, 462, 943
Ciucă I. et al., 2023, MNRAS
Cristallo S., Straniero O., Piersanti L., Gobrecht D., 2015, ApJS, 219, 40
da Silva R., Porto de Mello G. F., Milone A. C., da Silva L., Ribeiro L. S., Rocha-Pinto H. J., 2012, A&A, 542, A84
Delgado Mena E. et al., 2019, A&A, 624, A78
Delgado Mena E., Tsantaki M., Adibekyan V. Z., Sousa S. G., Santos N. C., González Hernández J. I., Israelian G., 2017, A&A, 606, A94
Feltzing S., Howes L. M., McMillan P. J., Stonkutė E., 2017, MNRAS, 465, L109
Frankel N., Rix H.-W., Ting Y.-S., Ness M., Hogg D. W., 2018, ApJ, 865, 96

Frankel N., Sanders J., Ting Y.-S., Rix H.-W., 2020, ApJ, 896, 15
Freeman K., Bland-Hawthorn J., 2002, ARA&A, 40, 487
Frischknecht U. et al., 2016, MNRAS, 456, 1803
García Pérez A. E. et al., 2016, AJ, 151, 144
Hayden M. R. et al., 2022, MNRAS, 517, 5325
Hayes C. R. et al., 2022, ApJS, 262, 34
Helmi A., Babusiaux C., Koppelman H. H., Massari D., Veljanoski J., Brown A. G. A., 2018, Nature, 563, 85
Holtzman J. A. et al., 2015, AJ, 150, 148
Jofré P., Jackson H., Tucci Maia M., 2020, A&A, 633, L9
Jönsson H. et al., 2020, AJ, 160, 120
Karakas A. I., Lattanzio J. C., 2014, Publ. Astron. Soc. Aus., 31, e030
Katime Santrich O. J., Kerber L., Abuchaim Y., Gonçalves G., 2022, MNRAS, 514, 4816
Kubryk M., Prantzos N., Athanassoula E., 2013, MNRAS, 436, 1479
Leung H. W., Bovy J., 2019, MNRAS, 483, 3255
Leung H. W., Bovy J., Mackereth J. T., Miglio A., 2023, MNRAS, 522, 4577
Lu Y., Minchev I., Buck T., Khoperskov S., Steinmetz M., Libeskind N., Cescutti G., Freeman K. C., 2022, preprint (arXiv:2212.04515)
Majewski S. R. et al., 2017, AJ, 154, 94
Matteucci F., 2021, A&AR, 29, 5
Matteucci F., Francois P., 1989, MNRAS, 239, 885
Minchev I. et al., 2018, MNRAS, 481, 1645
Minchev I., Chiappini C., Martig M., 2014, A&A, 572, A92
Minchev I., Famaey B., 2010, ApJ, 722, 112
Minchev I., Famaey B., Quillen A. C., Dehnen W., Martig M., Siebert A., 2012, A&A, 548, A127
Nissen P. E., 2015, A&A, 579, A52
Nissen P. E., 2016, A&A, 593, A65
Nissen P. E., Christensen-Dalsgaard J., Mosumgaard J. R., Silva Aguirre V., Spitoni E., Verma K., 2020a, VizieR Online Data Catalog, J/A + A/640/A81
Nissen P. E., Christensen-Dalsgaard J., Mosumgaard J. R., Silva Aguirre V., Spitoni E., Verma K., 2020b, A&A, 640, A81
Peña Suárez V. J., Sales Silva J. V., Katime Santrich O. J., Drake N. A., Pereira C. B., 2018, ApJ, 854, 184
Pilkington K. et al., 2012, A&A, 540, A56
Queiroz A. B. A. et al., 2023, A&A, 673, A155
Ratcliffe B. et al., 2023, MNRAS, 525, 2208
Ratcliffe B. L., Ness M. K., Buck T., Johnston K. V., Sen B., Beraldo e Silva L., Debattista V. P., 2022, ApJ, 924, 60
Ratcliffe B., Khoperskov S., Minchev I., Lu L., de Jong R. S., Steinmetz M., 2024, preprint (arXiv:2401.09260)
Rizzuti F., Cescutti G., Matteucci F., Chieffi A., Hirschi R., Limongi M., 2019, MNRAS, 489, 5244
Roškar R., Debattista V. P., Quinn T. R., Stinson G. S., Wadsley J., 2008, ApJ, 684, L79
Sales-Silva J. V. et al., 2022, ApJ, 926, 154
Schönrich R., Binney J., 2009, MNRAS, 399, 1145
Schönrich R., Binney J., Dehnen W., 2010, MNRAS, 403, 1829
Sellwood J. A., Binney J. J., 2002, MNRAS, 336, 785
De Silva G. M. et al. 2015, MNRAS, 449, 2604
Skúladóttir Á., Hansen C. J., Salvadori S., Choplin A., 2019, A&A, 631, A171
Slumstrup D., Grundahl F., Brogaard K., Thygesen A. O., Nissen P. E., Jessen-Hansen J., Van Eylen V., Pedersen M. G., 2017, A&A, 604, L8
Spina L., Meléndez J., Karakas A. I., Ramírez I., Monroe T. R., Asplund M., Yong D., 2016, A&A, 593, A125
Spitoni E. et al., 2021, A&A, 647, A73
Spitoni E. et al., 2023, A&A, 670, A109
Masseron T., Merle T. , Hawkins K., 2016, Astrophysics Source Code Library, record ascl:1605.004
Titarenko A., Recio-Blanco A., de Laverny P., Hayden M., Guiglion G., 2019, A&A, 622, A59
Tucci Maia M., Ramírez I., Meléndez J., Bedell M., Bean J. L., Asplund M., 2016, A&A, 590, A32
Van der Swaelmen M. et al., 2023, A&A, 670, A129
Vincenzo F., Kobayashi C., 2020, MNRAS, 496, 80
Viscasillas Vázquez C. et al., 2022, A&A, 660, A135

APPENDIX A: EXTRA PLOTS

Fig. A1 illustrates the metallicity distribution function of Model B compared to our GALAH DR3 sample. The median ±1 standard deviation values for each radial bin for our GALAH sample are as follows:

(i) 4 kpc: 0.01 ± 0.15
(ii) 6 kpc: -0.13 ± 0.16
(iii) 8 kpc: -0.26 ± 0.17
(iv) 10 kpc: -0.45 ± 0.20

The medians of Model B (4 kpc: −0.06, 6 kpc: −0.22, 8 kpc: −0.35, 10 kpc: −0.51) are within 1 standard deviation of the medians of the GALAH sample for each of the radial bins.

Fig. A2 gives a comparison of Model B to our GALAH DR3 sample for different birth radii bins.

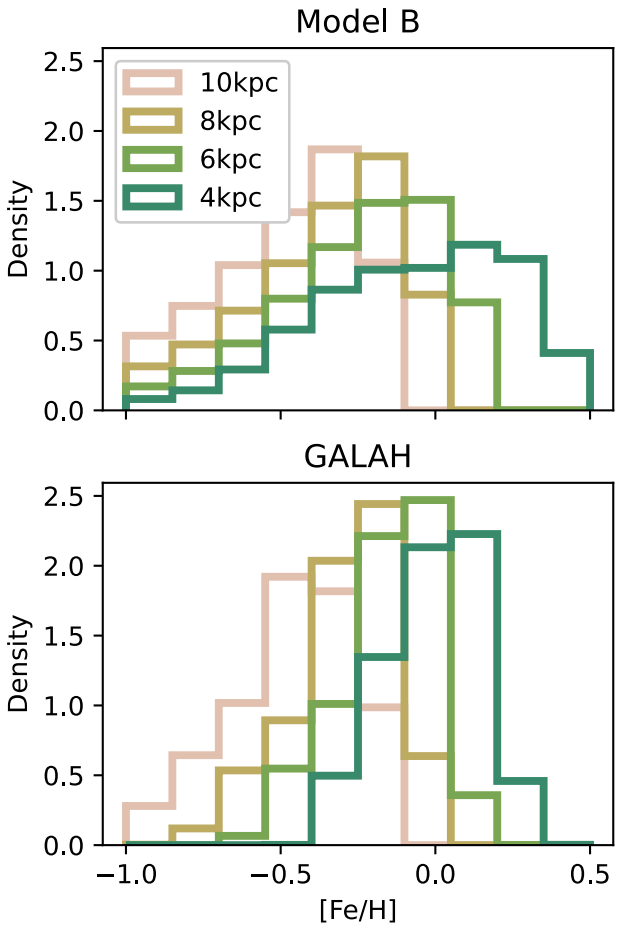

Figure A1. The metallicity distribution of *top*: Model B and *bottom*: our GALAH DR3 sample. The median values for each of the radial bins of Model B are within 1 standard deviation of the GALAH median values.

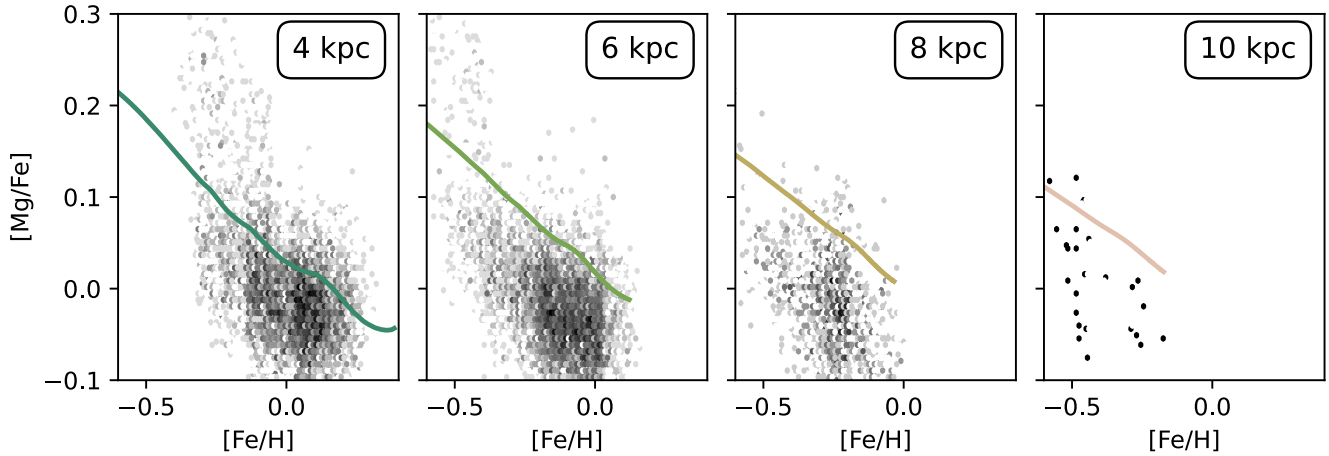

Figure A2. The [Mg/Fe]–[Fe/H] plane comparing Model B to GALAH DR3 data for different birth radii bins.

This paper has been typeset from a TEX/LATEX file prepared by the author.